Electronic Supplementary Material (ESI) for Physical Chemistry Chemical Physics.

Supplemental Information:

Coupled proton vibrations between two weak acids: the hinge complex between formic acid and trifluoroethanol

Sophie M. Schweer, Arman Nejad, and Martin A. Suhm*

Institute of Physical Chemistry, University of Göttingen, Tammannstr. 6, 37077 Göttingen, Germany.
E-mail: msuhm@gwdg.de

Contents

1 Computational modelling **S2**
1.1 Hybrid force field VPT2 . . . . . S2
1.2 Harmonic and VPT2 OH stretch scaling factors for B3LYP-D3 . . . . . S3
1.3 Harmonic spectroscopic properties S4
1.4 DFT minimum structures [6] S4

2 Experimental Data **S5**

References **S9**

1 Computational modelling

1.1 Hybrid force field VPT2

Different substituted hybrid force field approaches

It is common practice to express the higher derivatives of the potential energy (V) that enter into the VPT2 energy formulae [1, 2] as derivatives with respect to dimensionless normal coordinates ($\boldsymbol{q}$) as opposed to the usual mass-weighted rectilinear normal mode coordinates ($\boldsymbol{Q}$). This has the advantage that irrespective of the derivative order, all force constants ($\boldsymbol{\phi}$), i.e. derivatives of the potential energy, can be expressed in units of cm^{-1}. If the potential energy is expanded around a stationary equilibrium geometry, the Taylor series expansion (unrestricted summation) with respect to dimensionless coordinates has the form

$$V - V_{\mathrm{eq}} = \frac{1}{2}\sum_i \left.\frac{\partial^2 V}{\partial q_i^2}\right|_{\mathrm{eq}} q_i^2 + \frac{1}{6}\sum_{i,j,k} \left.\frac{\partial^3 V}{\partial q_i \partial q_j \partial q_k}\right|_{\mathrm{eq}} q_i q_j q_k + \ldots \tag{1}$$

$$= \frac{hc}{2}\sum_i \omega_i q_i^2 + \frac{hc}{6}\sum_{i,j,k} \phi_{i,j,k} q_i q_j q_k + \ldots, \tag{2}$$

where ω_i is the harmonic wavenumber. The conversion between the two coordinate systems equates to

$$q_i = \gamma_i^{1/2} Q_i, \tag{3}$$

with the conversion factor [3]

$$\gamma_i = \frac{hc\omega_i}{\hbar^2} = \frac{4\pi^2 c\omega_i}{h}. \tag{4}$$

which is not a constant but proportional to the harmonic wavenumber. When constructing a substituted hybrid force field as described in the supplementary material of Ref. [4], Gaussian 16 Rev. A.03 uses the *new* harmonic wavenumbers to evaluate $\boldsymbol{\gamma}$ (Eq. 4) and convert the cubic and quartic force constants from $\boldsymbol{Q}$ to $\boldsymbol{q}$ (Eq. 3).

Definition of effective resonance Hamiltonians

In order to identify near-degeneracies in the VPT2 treatment of the two OH stretching fundamental energy levels of the 1:1 complex between T_g and F, the well-tried Martin test is employed [5]. We use default thresholds as implemented in Gaussian 16 Rev. A.03 (harmonic energy separation $\leq 200\,\mathrm{cm}^{-1}$ and variational-perturbational difference $\geq 1\,\mathrm{cm}^{-1}$) and restrict the resonance treatment to Fermi resonances (VPT2+F) following the usual procedure of deperturbation (indicated by an asterisk) and subsequent diagonalisation of effective resonance Hamiltonians as described for example in Ref. [2]. Indeed, a Fermi resonance is detected between the higher-frequency alcoholic stretch (ν_1) and a combination state which is excited along the lower-wavenumber acidic stretch (ν_2) and a low-frequency mode (ν_{33}) shown below:

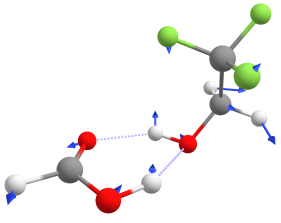

ν_{33} is an intermolecular vibrational degree of freedom (or frustrated rotation) which is a mixed group vibration with partial OH libration character (and internal rotation along the CC bond) which makes ν_1 and ν_2+ν_{33} quite natural coupling partners. The corresponding 2×2 VPT2+F Hamiltonian has the following form:

$$\frac{\mathbf{H}_{\mathrm{eff}}}{hc} = \begin{pmatrix} (\nu_1)^* & \frac{1}{2\sqrt{2}}\phi_{1,2,33} \\ \frac{1}{2\sqrt{2}}\phi_{1,2,33} & (\nu_2{+}\nu_{33})^* \end{pmatrix} \tag{5}$$

Results and discussion

Differently computed energy levels of both OH stretching vibrations of the 1:1 complex between T and F are summarised in Table S1, illustrating the impact on the energy levels for different hybrid force field approximations and the explicit resonance treatment between ν_1 and ν_2+ν_{33}. In the limit of a single bright state, the fundamental character

Table S1: Comparison of computed (harmonic and anharmonic VPT2) and experimental energy levels (in cm^{-1}) of the acidic (ν_2) and alcoholic (ν_1) OH stretching vibrations and ν_{33} of (T_g^gF). ν_1 is predicted to be in resonance with $\nu_2+\nu_{33}$ and the squared wavefunction contribution from the deperturbed fundamental (c_1^2) is shown for a two-level analysis (Eq. 5). "add" and "sub" refer to the additive and substituted hybrid force field approach, respectively, where "mod" additionally indicates that the cubic and quartic force constants are scaled as described in the text. Δ_{OH} is the difference between the two OH stretching fundamentals and Δ_{res} between the two resonant levels.

$CF_3CX_2OH \cdot HCOOH$			ν_{33}	ν_2	ν_1	c_1^2	$\nu_2+\nu_{33}$	$1-c_1^2$	Δ_{OH}	Δ_{res}
X = H	harmonic	MP2/aVTZ	133	3451	3562		3584		111	22
X = H	harmonic	CCSD(T)-F12a/VDZ-F12	131	3515	3614		3645		100	31
X = H	VPT2	MP2/aVTZ	127	3245	3347		3383		102	36
X = H	VPT2	hybrid(add)	124	3309	3399		3444		90	45
X = H	VPT2	hybrid(sub,mod)	124	3315	3411		3447		96	36
X = H	VPT2	hybrid(sub)	124	3302	3399		3434		97	35
X = H	VPT2+F	MP2/aVTZ			3348	0.77	3381	0.23	103	33
X = H	VPT2+F	hybrid(add)			3400		3443		92	42
X = H	VPT2+F	hybrid(sub,mod)			3411	0.82	3447	0.18	95	36
X = H	VPT2+F	hybrid(sub)			3398	0.81	3434	0.19	97	36
X = H	experiment	FTIR		3309	3408		3441?		99	33?
X = D	harmonic	MP2/aVTZ	127	3451	3562		3577		111	16
X = D	harmonic	CCSD(T)-F12a/VDZ-F12	124	3515	3614		3639		100	25
X = D	VPT2	hybrid(sub)		3301	3399		3425		98	26
X = D	VPT2+F	hybrid(sub)			3397	0.68	3427	0.32	96	29

(c_1^2 and $1-c_1^2$) reflects the intensity ratio to be expected for the resonance doublet. To lowest-order, the Fermi coupling constant is $(2\sqrt{2})^{-1}\phi_{1,2,33} = 14\,cm^{-1}$ at the MP2/aVTZ level. The impact of this resonance on the energy levels is negligible (deviation between VPT2 and VPT2+F is only 1-2 cm^{-1}) but the mixing between both states is quite strong, as reflected in the fundamental character of the perturbed $\nu_2+\nu_{33}$ state (see Table S1). The data presented in Table S1 support a speculative assignment of the weak IR band at 3441 cm^{-1}, which could find several possible experimental interpretations, to the combination state $\nu_2+\nu_{33}$. They also suggest that this assignment option has little impact on the theory-experiment comparison for the fundamental wavenumbers, which is most relevant for this work. We note that full CH_2 deuteration might yield further insights into the assignment of the IR band at 3441 cm^{-1} as the proposed resonance between ν_1 and $\nu_2+\nu_{33}$ is not only predicted to survive but even increase in strength, as indicated by the decrease of c_1^2 (Table S1).

1.2 Harmonic and VPT2 OH stretch scaling factors for B3LYP-D3

Table S2: Scaling factors (x, in %) derived for the OH stretching fundamentals (ω and $\tilde{\nu}$, in cm^{-1}) of the global minimum structures of formic acid F, trifluorethanol T_g and their mixed 1:1 complex (T_g^gF). Note that at the coupled-cluster level, the anharmonic VPT2 correction is computed at the MP2/aVTZ level following the substituted hybrid force field approach, as described in Section 2.3 of the main text. Column D shows that the latter are in almost perfect agreement with experiment. Therefore, the empirical B3LYP harmonic scaling by 96% (column A) is seen to be the result of 94-95% scaling for pure anharmonicity (column C) and a 1-2% correction for the harmonic deficiency of the B3LYP approach, namely an OH bond which is somewhat too soft, both in the monomer and even more so in the complex.

	Exp.	B3LYP-D3/def2QZVP				CCSD(T)-F12a/VDZ-F12			
	FTIR	Harmonic		VPT2		Harmonic		VPT2	
	$\tilde{\nu}_{exp}$	ω_{harm}	x_{harm}	$\tilde{\nu}_{VPT2}$	x_{VPT2}	ω_{harm}	x_{harm}	$\tilde{\nu}_{VPT2}$	x_{VPT2}
			A		B		C		D
F	3570	3727	95.8	3537	100.9	3759	95.0	3575	99.9
T_g	3656	3818	95.8	3636	100.6	3839	95.2	3662	99.8
(T_g^gF)	3309	3436	96.3	3222	102.7	3515	94.2	3302	100.2
(T_g^gF)	3408	3546	96.1	3319	102.7	3614	94.3	3399	100.3

1.3 Harmonic spectroscopic properties

Table S3: Spectroscopic properties (harmonic OH stretching wavenumber ω_{OH}, downshifts relative to the respective T and F monomer $\Delta\omega_{OH}$ (T/F), infrared band strength S_ω, Raman cross section σ_{Raman} corrected for instrument properties and energies, relative conformational energy ΔE_0 and dissociation energies $D_{e/0}$ without and with zero point energy correction into the respective monomer structures for different species optimized at the B3LYP-D3(BJ)/def2-QZVP level. Structures are shown in Figure S1 and Figure S2.

Structure	ΔE_0	ω_{OH}	$\Delta\omega_{OH}$ (T/F)		S_ω	σ_{Raman}	D_e	D_0
	kJ mol^{-1}	cm^{-1}	cm^{-1}		km mol^{-1}	10^{-35}m^2	kJ mol^{-1}	kJ mol^{-1}
F	-	3727	-		60	6.64	-	-
(FF)	-	3156	-	571	2166	0	73.8	66.2
		3030	-	697	0	26.1		
T_g	-	3818	-		49	4.97	-	-
T_t	-	3850	-		57	7.33	-	-
T_gT_g	-	3792	26	-	127	3.95	31.1	26.3
		3673	145	-	429	10.9		
(T_g^gF)	0	3546	272	181	741	3.73	44.7	38.0
		3436	382	291	269	17.3		
(T_g^tF)	1.80	3572	246	155	607	5.37	42.8	36.2
		3407	411	320	481	19.4		
T_gF	4.89	3816	2	−89	62	5.81	38.4	33.1
		3431	387	296	750	14.3		
T_gF'	5.30	3661	157	66	536	4.89	38.2	32.7
		3609	209	118	436	17.3		

1.4 DFT minimum structures [6]

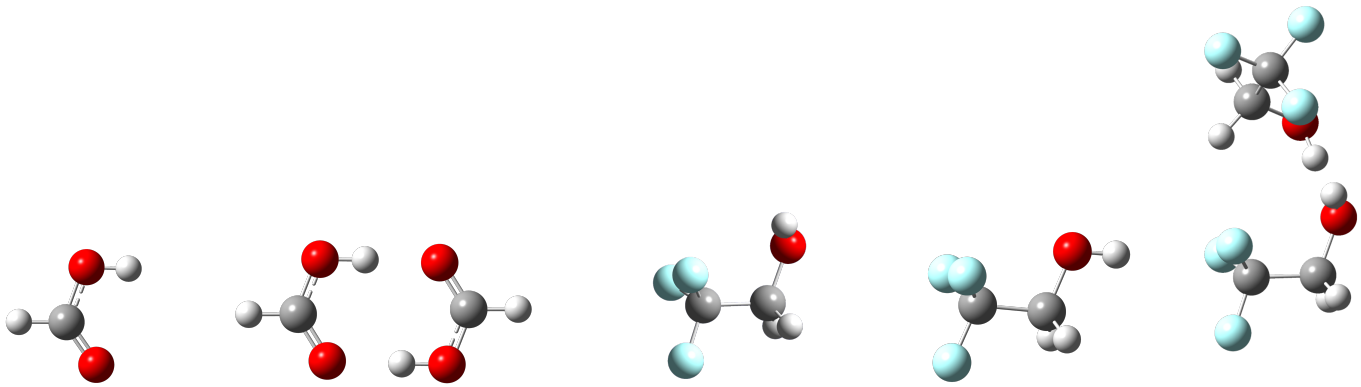

Fig. S1: Most stable structures of the monomers and the most stable dimers of pure trifluoroethanol and formic acid, optimized at the B3LYP-D3(BJ)/def2-QZVP level. For T_g the respective g+ enantiomer is shown and for its dimer, homochirality is implied.

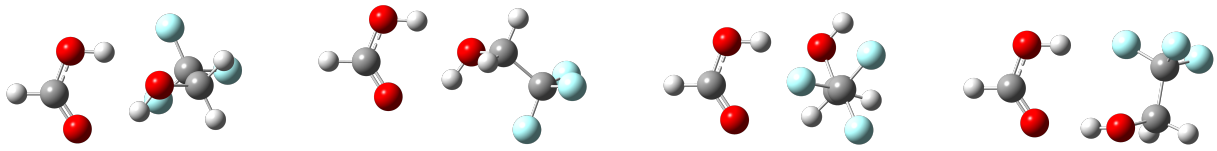

Fig. S2: Most stable structures of mixed dimers of trifluoroethanol and formic acid, optimized at the B3LYP-D3(BJ)/def2-QZVP level. The energy difference with respect to the global minimum structure (a) is included. For the complexes containing T_g, the respective g+ enantiomer is shown. The compact name starts with the (preferentially alcohol) donor, backbinding is indicated with parentheses. A g/t superscript denotes the alcohol lone pair for backbinding.

2 Experimental Data

Table S4: Experimental details for the shown FTIR jet spectra. Each spectrum was recorded with an aperture of 3.5 mm, an InSb/MCT sandwich detector, a spectral bandpass filter transparent between 2500 and 4100 cm^{-1} (internal reference: F13a), CaF_2 optics and a resolution of 2 cm^{-1}. The helium pressure in the gas pipes (p_{He}) and the reservoir pressure (p_{Res}) are listed. For each measurement, a mixed-gas bottle with defined concentrations was prepared, e.g. for the purple spectrum, 10 mbar formic acid (F) was mixed with 20 mbar of 2,2,2-trifluoroethanol (T) within 50 bar He. 'F : T in 50 bar He' shows the individual conditions. The spectra were averaged over multiple scans, with N_{Scan} as the amount of averaged scans. The date the spectra were recorded as well as the filename are listed for internal reference. The raw data for the spectra are publicly available [6].

Figure	Trace	p_{He}	p_{Res}	F : T in 50 bar He	N_{Scan}	Date	Filename
		bar	bar	mbar		YY:MM:DD	
1 S3 S4	b, blue b, blue a, blue	1.6	0.75	– : 20	365 (5+145+100+100+15)	19:08:19	190819-a-TFE-[...].365.dpt
1 S3 S4	a, red a, red b, red	1.6	0.75	10 : –	375 (5+20+125+150+50+25)	19:08:29	190829-a-FA-[...].375.dpt
1 S4	c, light purple e, light purple	1.6	0.75	10 : 10	360 (5+45+150+200+50+10)	19:09:02	190902-a-FA-[...].360.dpt
1 S3 S4	c, purple c, purple d, purple	1.6	0.75	10 : 20	360 (5+245+100+10)	19:09:10	190910-a-FA-[...].360.dpt
1 S4	c, pink c, pink	1.6	0.75	20 : 20	365 (5+45+150+100+50+15)	19:08:15	190815-a-TFE-[...].365.dpt

Table S5: Experimental details for the shown Raman jet spectra. Each spectrum was recorded with 2.0 bar helium pressure at the saturators, 0.7 bar reservoir pressure and the feeding lines and nozzle at room temperature. The laser beam (532.274 nm, 25 W) crossed the expansion with a distance of 1 mm to the nozzle. The monochromator was set at 647.2 nm and every spectrum is averaged over 10 scans with an exposure time of 600 s each. The saturator temperatures for formic acid (F, θ_F) and 2,2,2-trifluoroethanol (T, θ_T) are listed. For the generation of the gas mixture, gas flow meters were used. 'F (in He) : T (in He) : He' shows the individual flow meter settings for internal reference. For calibration and conversion to wavenumbers, atomic transitions of a neon and partly also a krypton discharge lamp were used ('Calib'). The date the spectra were recorded as well as the filename are listed for internal reference. Note to reviewer: the spectra will be made available as data point tables in a public repository at revision stage.

Figure	Trace	θ_F	θ_T	F (in He) : T (in He) : He	Calib	Date	Filename
		° C	° C			YY:MM:DD	
2 S5	a, red a, red	10	–	5 : 100 (He) : 50	Ne&Kr	21:10:06	20211006_a_He_[...]_des_avg_cal.dat
2 S5	b, blue b, blue	–	−25	5 (He) : 100 : 50	Ne&Kr	21:10:05	20211005_b_TFE_[...]_des_avg_cal.dat
2 S5	c, blue e, blue	10	−25	5 : 100 : 5	Ne	21:07:06	20210706_b_FA_[...]_des_avg_cal.dat
2 S5	c, pink d, pink	10	−25	10 : 50 : 50	Ne	21:07:06	20210706_d_FA_[...]_des_avg_cal.dat
2 S5	c, purple g, light purple	10	−25	5 : 50 : 50	Ne&Kr	21:10:05	20211005_a_TFE_[...]_des_avg_cal.dat
S5	c, purple	10	−25	10 : 100 : –	Ne	21:07:06	20210706_a_FA_[...]_des_avg_cal.dat
S5	c, red	10	–	10 : 100 (He) : –	Ne	21:07:06	20210706_c_FA_[...]_des_avg_cal.dat
S5	c, blue	–	−25	– : 100 : –	Ne	21:10:05	20210707_a_TFE_[...]_des_avg_cal.dat
S5	f, light purple	10	−25	5 : 50 : 55	Ne	21:07:09	20210709_b2_FA_[...]_des_avg_cal.dat

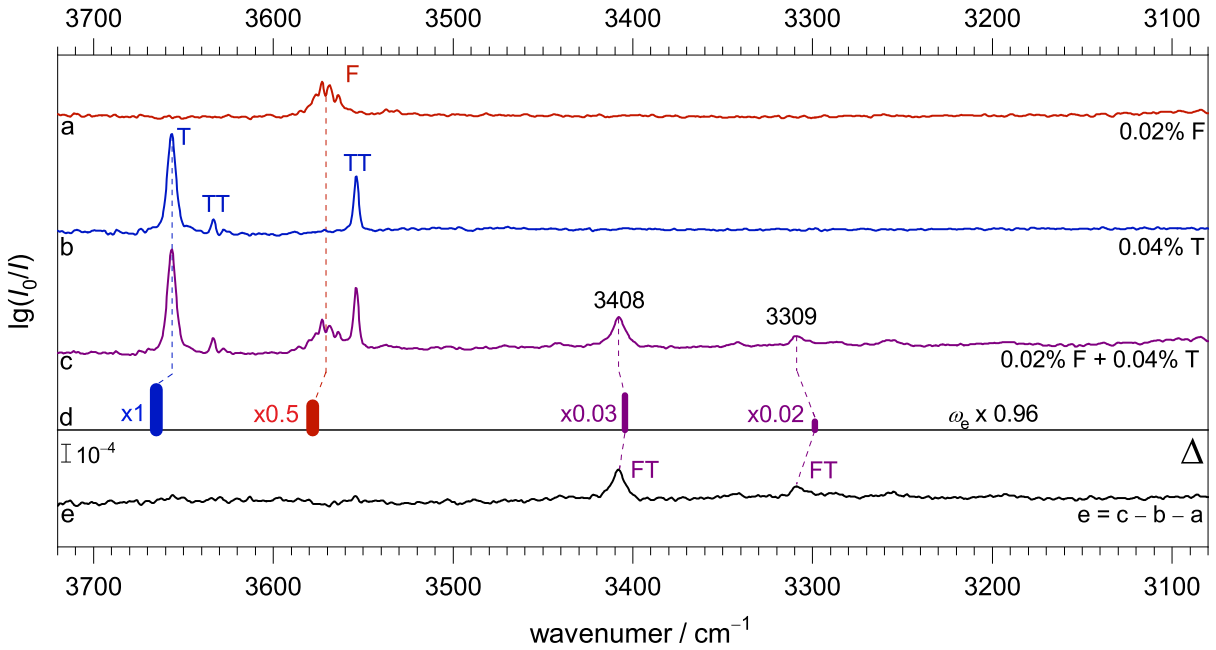

Fig. S3: Estimate of the fraction of 1:1 complexes relative to the monomer ingredients in the spectra based on computed harmonic infrared intensities and a comparison of relative experimental intensities, as reflected by the scaling factors applied to the simulated spectra (trace d) to qualitatively match experiment (trace e, obtained by subtracting the one-component spectra a and b from the spectrum c of the mixture). The 1:1 complex is seen to involve more than 1% and significantly less than 10% of the molecules in the expansion, even allowing for substantial uncertainties in the theoretical intensities.

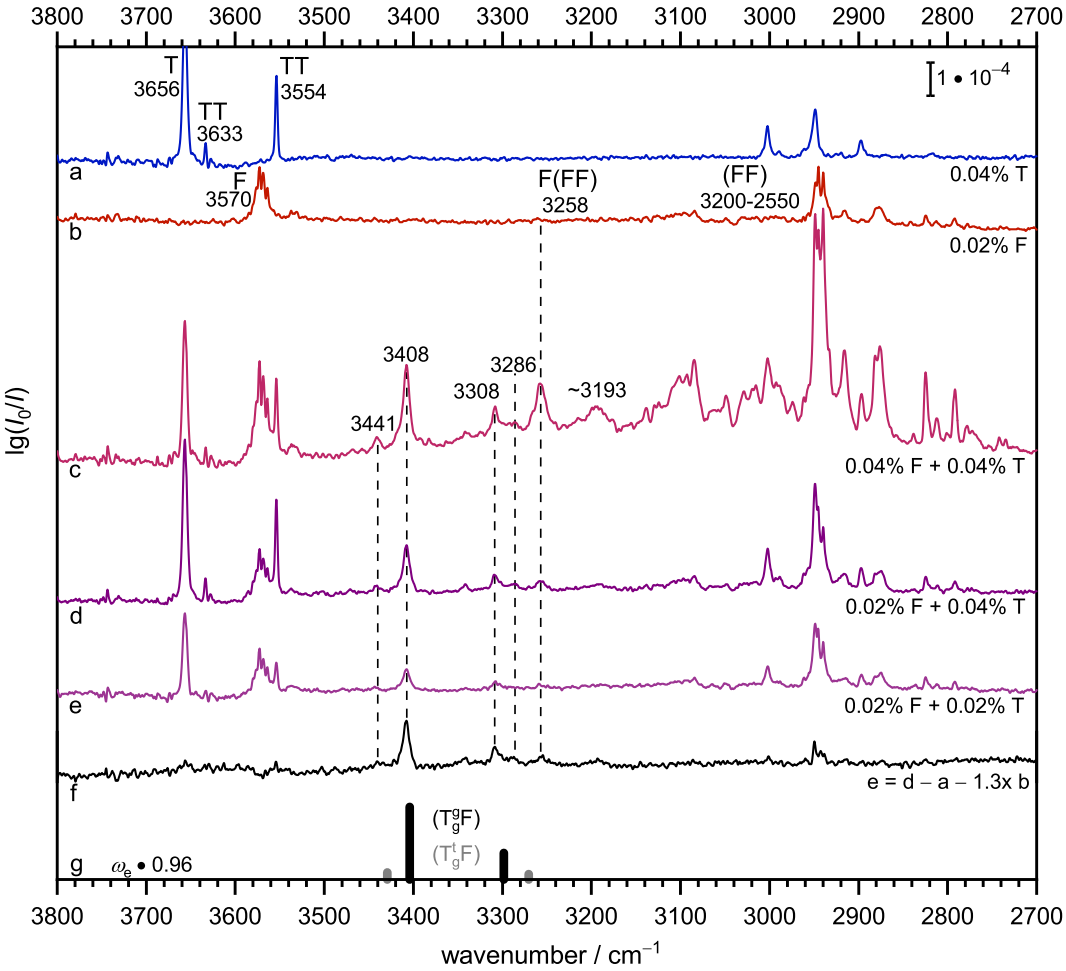

Fig. S4: FTIR spectra of 2,2,2-trifluoroethanol in helium (a), formic acid in helium (b) and premixed mixtures of both with different concentrations in helium (c,d,e). Additionally, a difference spectrum (f) for trace e is shown, which was obtained by subtracting scaled single substance spectra from that of the mixture. At the bottom (g) harmonically calculated (B3LYP-D3(BJ)/def2QZVP), scaled (0.96) band positions of the OH-stretching vibrations for (T_g^gF) (black) and (T_t^gF) (grey) are shown assuming a 100 K Boltzmann distribution.

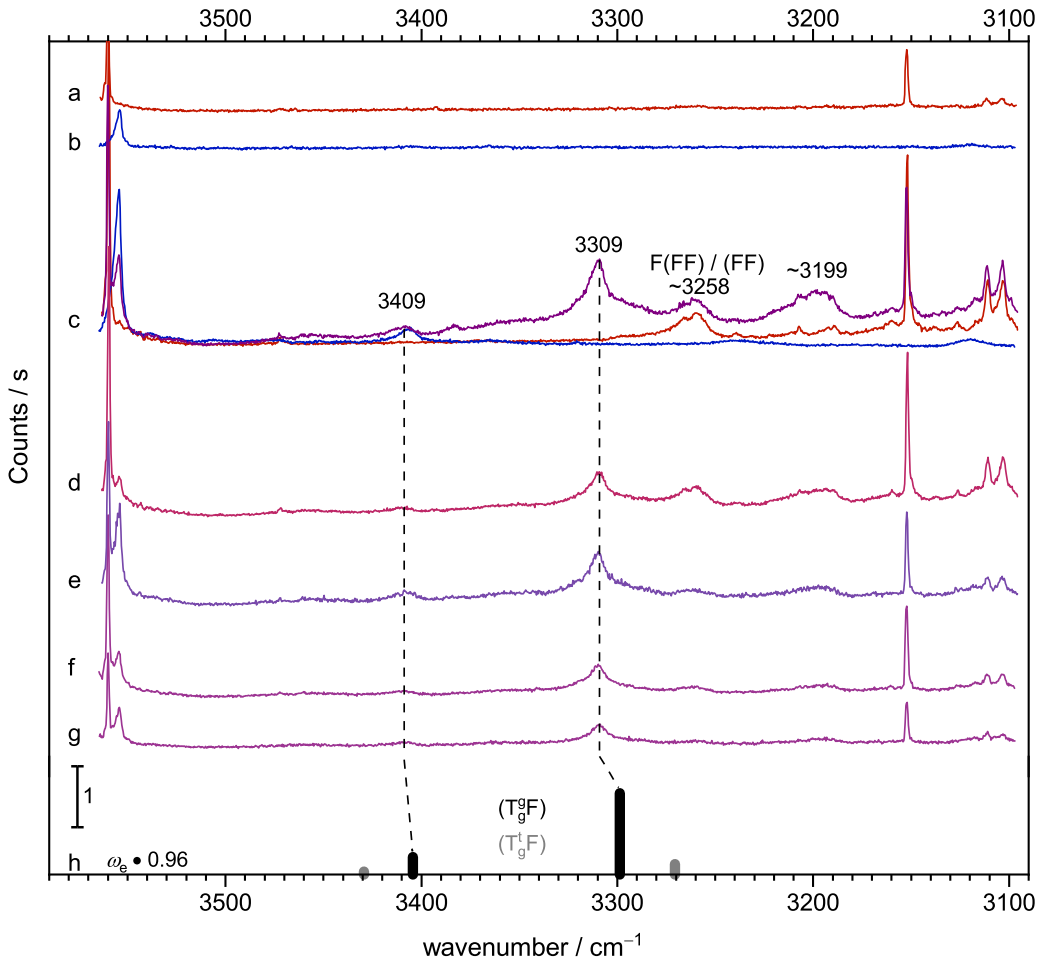

Fig. S5: Raman spectra of formic acid in helium (a), 2,2,2-trifluoroethanol in helium (b) and mixtures of both with different concentrations in helium (c-g). Additionally, in trace c corresponding pure substrate spectra are shown (T in blue, F in red). At the bottom (h) harmonically calculated (B3LYP-D3(BJ)/def2QZVP), scaled (0.96) band positions of the OH-stretching vibrations for (T_g^gF) (black) and (T_t^gF) (grey) are shown assuming a 100 K Boltzmann distribution.

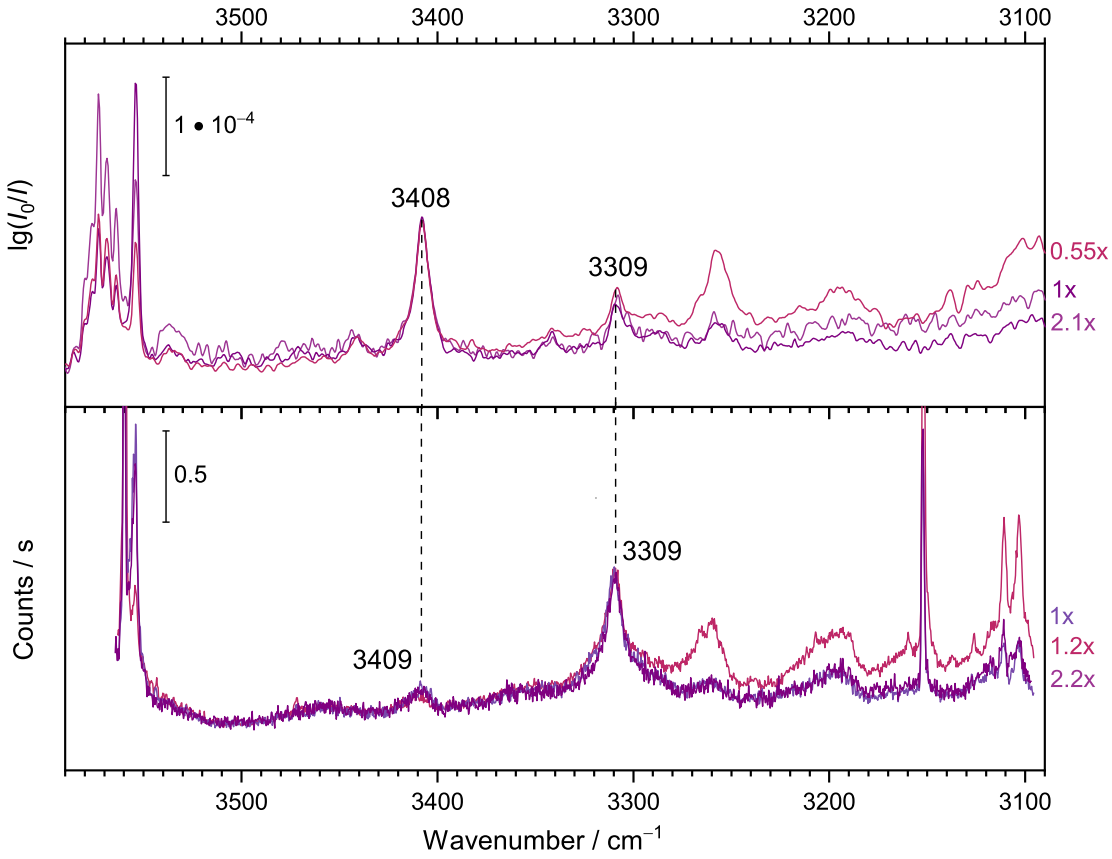

Fig. S6: Direct comparison between the scaled FTIR and scaled Raman spectra from Fig. 1, trace d (IR) and Fig. 2, trace d (Raman), respectively. Easy to see is the switch of the intensity pattern: While the alcoholic OH-stretching vibration at 3408/9 cm^{-1} has a high IR and a low Raman intensity, the pattern is changed for the acidic OH-stretching vibration at 3309 cm^{-1}.

References

[1] H. H. Nielsen, *Rev. Mod. Phys.* **1951**, *23*, 90–136.

[2] P. R. Franke, J. F. Stanton, G. E. Douberly, *J. Phys. Chem. A* **2021**, *125*, 1301–1324.

[3] E. B. Wilson Jr., J. C. Decius, P. C. Cross, *Molecular Vibrations: The Theory of Infrared and Raman Vibrational Spectra*, Dover Publications Inc., New York, **1980**.

[4] A. Nejad, K. A. E. Meyer, F. Kollipost, Z. Xue, M. A. Suhm, *J. Chem. Phys.* **2021**, *155*, 224301.

[5] J. M. L. Martin, T. J. Lee, P. R. Taylor, J. François, *J. Chem. Phys.* **1995**, *103*, 2589–2602.

[6] M. A. Suhm, S. M. Schweer, A. Nejad, **2022**, DOI 10.25625/I67U1B.